Chem. Chem. Technol., 2024,
Vol. 18, No. 3, pp. 401–408

Chemical Technology

CHOLESTERIC LIQUID CRYSTAL MIRROR-BASED SMART WINDOW CONTROLLED WITH AMBIENT TEMPERATURE

Gia Petriashvili[1,✉], Tamaz Sulaberidze[1], David Tavkhelidze[2], Mikheil Janikashvili[2], Nino Ponjavidze[1], Andro Chanishvili[1], Ketevan Chubinidze[1], Tamara Tatrishvili[3,4], Tamar Makharadze[1], Elene Kalandia[1], Khatuna Tserodze[1], Riccardo Barberi[5], Maria Penelope De Santo[5]

https://doi.org/10.23939/chcht18.03.401

Abstract. In this paper, the authors demonstrate a small prototype of a smart window based on the thermo-optical properties of cholesterol liquid crystals. Due to its polymer-free design, the manufactured smart window is transparent and can reflect certain portions of visible or infrared light without requiring an external power source, and thus is easier to install and operate. The proposed smart window technology based on a cholesteric liquid crystal mirror will reduce energy consumption costs by reflecting excess sunlight and heat transfer, increasing comfort for residents of buildings and structures.

Keywords: smart windows, cholesteric liquid crystals, temperature controlled, light reflection.

1. Introduction

High energy consumption has attracted global attention and sparked interest in new energy sources, energy conservation, and methods to reduce energy costs. The buildings segment accounts for 40 % of global energy demand, and ventilation, heating and air conditioning account for half of the energy consumption in buildings[1,2]. Increasing or decreasing the intensity of light coming in through windows can have a significant impact on a country's overall energy consumption. Due to temperature fluctuations throughout the day or season, the amount of solar radiation reaching the building can be controlled by using windows that control the intensity of incoming visible and infrared light. In this way, it is possible to let solar energy into the building if more heat is needed, and it is possible to reduce the passage of solar energy into the building if cooling is needed[3–5]. Controlling the intensity of incoming light and solar energy can be achieved using materials with variable optical properties. These materials are called chromogenic and are capable of reversible or irreversible color change when exposed to external or internal stimuli such as heat, electric field, pressure, or light[6, 7]. Three basic types of chromism are used in energy-associated applications, such as photo-chromism, thermochromism, and electrochromism. Photochromism characterizes the irradiation-stimulated reversible conversion of a material's color between two conditions[8]. During the reversible phototransformation, several physical parameters of photochromic compounds can be modified by light, such as electron conductivity, fluorescence emission, absorption and transmission spectra, conjugation, electrochemical and magnetic behavior, coordination properties, dipole interactions, dielectric constant, refractive index, and geometrical structure[9, 10]. Generally, thermochromism describes the variation in a material's color due to a temperature change, which is determined as a reversible or irreversible process[11]. Electrochromism implies a reversible change in transmittance and reflectance associated with an oxidation-reduction reaction, which electrochemically is induced. Electrochromic devices have progressively been investigated for energy-saving smart windows and displays for airplanes, automobiles, and buildings[12, 13]. The smart windows belong to the systems that can sense and react to external stimuli such as electricity, heat, or light, which controls the light passing through the glass. Even though smart windows composed of these materials have the advantages of flexible switching speed and high color contrast, the high cost of material synthesis, low response

[1] Vladimir Chavchanidze Institute of Cybernetics of the Georgian Technical University, 5, Z. Andjzaparidze str., Tbilisi, 0186, Georgia
[2] Georgian Technical University, M. Kostava str., 77, Tbilisi 0171, Tbilisi, Georgia
[3] Ivane Javakhishvili' Tbilisi State University, Department of Macromolecular Chemistry, 1, I. Chavchavadze Ave., Tbilisi, 0179, Georgia
[4] Institute of Macromolecular Chemistry and Polymeric Materials, Ivane Javakhishvili Tbilisi State University, 2, University St Tbilisi, 0186, Georgia
[5] CNR-IPCF, UOS Cosenza, Physics Department, University of Calabria, Rende (Cs), 87036, Italy
✉ *g.petriashvili@yahoo.co.uk*

time, and insufficient stability limit their practical applications. For instance, windows manufactured of photochromic materials are vulnerable to losing effectiveness over time due to photochemical decomposition and darkening on a cold sunny day when more solar heat is needed[14, 15]. In recent years, growing ecological and environmental awareness has spurred efforts to develop new composites derived from organic materials such as polymers, thermoplastics, and liquid crystals[16–20]. Liquid crystals are the intermediate (mesomorphic) state between the solid and liquid phase conditions. They are composed of such chemical compounds as bicyclohexane, difluoro alkoxy-cyclohexane-biphenyl, pentylphenyl, pentybenzoate, biphenylcarbonitrile, azoxydianisole, azoxyanisole, methylbenzene, *etc*. Among the advanced materials granted with the selective reflection of light are the cholesteric liquid crystals (CLCs) consisting of chiral organic molecules. The CLC phase is a mesomorphic structure with a self-aligned periodical helical order that acts as a one-dimensional periodic system. In planes perpendicular to the helical axis, the molecules have a favored average orientation characterized by the so-called director. Due to their optical properties, CLCs are considered one-dimensional photonic crystals. Broadband cholesteric liquid crystals (CLCs) have many applications for reflective polarizers and displays. The period of the CLC structure is proportional to half the pitch P_0 of the helix. For light movement along the helical axes, $P_0 = \lambda_0/n$, where λ_0 is the middle point of the maximum selective reflection band (SRB), and n is the average value of the refractive indices defined as $n = (n_e + n_o)/2$. Its full width determines the SRB of a CLC at half maximum $\Delta\lambda = P_0\Delta n$, where $\Delta n = n_e - n_o$ is the birefringence of the nematic liquid crystal layer perpendicular to the helix axis. Stimuli that can modify the SRB in CLC include temperature, light, electric field, dopant concentration, mechanical deformation, two-photon polymerization, chemical substances, bio-molecules, pH changes, and humidity[21–28]. When non-polarized light hits the CLC structure parallel to the helical axis, it reflects half of it and transmits the other half, acting like a reflective mirror[29]. Smart windows made of thermochromic or photochromic liquid crystals are attracting attention for their ability to modulate the transmittance according to the environment. For instance, it outlines an electrically switchable CLC-based window that can alternate between a clear and diffuse state. The transparent state displays a well-ordered planar cholesteric texture and remains stable without an electric field[30]. The diffuse condition is activated by applying an electric field above the undulation instability threshold. Tseng *et al*.[31] demonstrated a smart window with photochromic dye and salt-doped CLC.

In this work, we propose a new fabrication method for CLC mirror-based smart window (CLCSW) that can reflect visible or infrared light without applying an external power source. Moreover, the CLCSW can respond to the environmental temperature to independently rearrange a light reflection, which can be easily adjusted to daylight time and climate regions. Here, we mention the recent progress made in developing advanced LC-based smart windows described by several authors[32–34], where different advanced LC-based smart window technologies and new classes of light modulation principles are demonstrated based on liquid crystal materials and their feasibility of using them for light protection, including electrochromism, thermochromism, photochromism, humidity-triggered chromism, mechanical self-powered technique, guest-host liquid crystal cells by introducing a novel design featuring a uniform lying helix structure and dynamic infrared regulating mechanisms. However, the smart windows we present are different from those currently in use or being researched because our windows do not contain polymers or dyes, which leads to such advantages as high transparency, efficiency, photostability, and operational durability.

2. Experimental

2.1. Materials and Equipment

The CLC mixture was prepared by mixing two initial materials. A left-handed chiral agent, 4-[1-methylheptyloxy] carbonyl phenyl-4-(hexyloxy) benzoate (ZLI-811), was doped in the nematic matrix BL-036, which is a blend of alkylcyanobiphenyls compounds. The resulting mixture was composed of BL-036 (74.5 wt. %) and ZLI-811 (25.5 wt. %). All materials were purchased from Merck. The refractive indices of BL-036 are $n_e = 1.794$ and $n_o = 1.5270$, with an optical birefringence $\Delta n = 0.2670$ at $T = 20$°C and $\lambda = 589$ nm. The mixture was uniformly stirred for 15 min in the isotropic phase at 100 °C to obtain the evenly mixed composite. For the preparation of the CLC mixture, a digital analytical balance with 0.1 mg accuracy was used. An imaging-based technique, consisting of an optical microscope coupled with a fiber-optic spectrometer (Avaspec-2048, Avantes) with 1 nm accuracy and a high-resolution CCD camera, was used to visually and graphically present the light transmitted through and reflected from the CLC. The visible-near-infrared solar power meter (TES 132) was used to measure light intensity in the range of 350–1000 nm of the optical spectrum, displaying solar irradiance in mW/cm^2. The temperature dependences of the SRBs of the CLC mixtures were controlled by a hot stage with a 0.1 °C accuracy.

2.2. Assembling of the Optical Cell

A small optical cell was assembled to record the temperature-dependent tuning of SRBs of the CLC. Two glass plates with a 2×2 cm area each were treated in deionized water and coated with a thin layer of polyvinyl alcohol (PVA, from Sigma-Aldrich) using a spin-coating technique. The glass plates were dried in the oven at 80 °C for 60 min to remove water and then rubbed in opposite directions for planar alignment of the CLC material. The distance between the plates was set at 8 μm using Teflon films. The CLC mixture was infiltrated by capillarity into an optical cell in the isotropic phase, which was then inserted into a hot plate and placed under an optical microscope connected to a spectrometer.

2.3. Fabrication of the CLCSW

Two 8×8 cm glass plates were used to fabricate a small CLCSW. The plates were preliminarily double-cleaned with deionized water. PVA solution was cast by dropping it on the glass substrates, dried in the oven for 60 min at 80 °C, and then rubbed in opposite directions. Precise control of the gap thickness is crucial to achieving the best CLCSW performance. For this purpose, plastic spacers of 8 μm made of highly crosslinked monodisperse polymer microspheres were used. Spacers were deposed on glass plates using wet spray-coating technology. In particular, the plastic spacers were ultrasonicated in an ethanol / water solution (40:60, w/w) and then sprayed on the glass substrates. Plates were placed in the drying chamber at 60 °C for 24 h. Before the CLC mixture infiltration inside the optical cell, plates were assembled and sealed using a UV-curing procedure, Fig. 1.

The assembled cell was filled with CLC by capillarity, taking care to avoid bubbles/gaps near the boundaries, and examined under a polarizing microscope to confirm the correct alignment of the director. Fig. 2, *a* shows a CLCSW with a uniformly aligned CLC mixture, and Fig. 2, *b* shows a schematic cross-section of a CLCSW, where the plastic spacers are used to keep the constant distance between the glass plates.

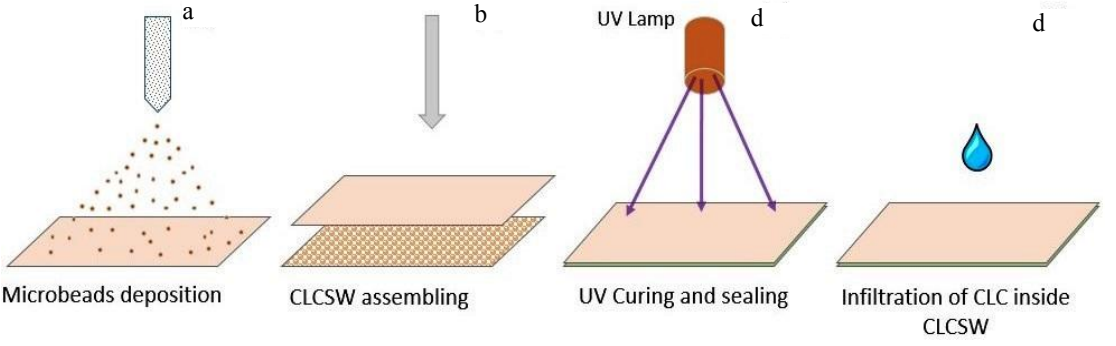

Fig. 1. Schematic image the of CLC-based smart window fabrication: spray coating over the transparent glass substrate with microbeads (a), assembling the optical cell with a fixed 8 μm gap (b), UV curing and sealing of the optical cell (c), infiltration of optical cell with the CLC (d)

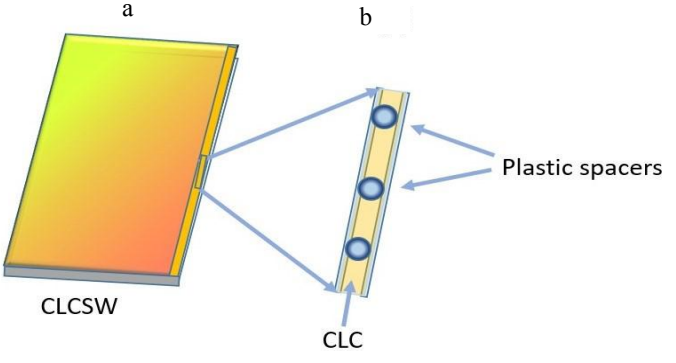

Fig. 2. An assembled CLCSW (a) and the spacers used to fix the gap between the glass plates so that the CLC substance can be injected evenly inside CLCSW (b)

3. Results and Discussion

To investigate the temperature-dependent shifting of SRBs of the CLC, we built a setup shown in Fig. 3. The left part of Fig. 3 shows the experimental devices and the right side of Fig. 3 shows the microscopic images of the CLC mixture at different temperatures captured by a CCD camera. As seen from the picture, at 20 °C the CLC mixture reflects the red part of the optical spectrum, at 30 °C – the yellow-orange part, and at 35 °C – the green part.

Using a spectrometer, we recorded the temperature-dependent tuning of SRBs of the CLC when heated (Fig. 4). In the experiments, the thermal tuning of SRBs was recorded starting at +10 °C, where the central wavelength of the SRBs of CLCs is located at $\lambda = 750$ nm of the optical spectrum and reaches $\lambda = 545$ nm at 35 °C. However, the temperature interval of the CLC phase existence is much broader, between –12 °C and +80 °C. As the temperature increases, the blue-shifting of SRBs takes place. It should be noted that the sequence of spectral changes in the SRB is the same when heated and cooled.

Fig. 4, *b* shows the dependence of temperature tuning of the SRBs of the CLC at low temperatures, which is negative, a $\partial P/\partial T < 0$, and this dependence becomes zero at high temperatures, a $\partial P/\partial T = 0$. In particular, the SRBs no longer shift when the ambient temperature is 35 °C or higher. At these temperatures, the SRBs reflect the 520–580 nm spectral range of solar radiation, which coincides with the maximum intensity emitted by the sun.

The second part of the experiments was carried out using the CLCSW. Fig. 5, *a*, *b* demonstrates the operation principle of the CLCSW. The CLCSW is transparent at low temperatures and transmits solar radiation inside the building. As the temperature increases, the SRBs shift towards the visible part of the optical spectrum and reflect the most intense portion of the solar radiation when the selective reflection no longer moves spectrally.

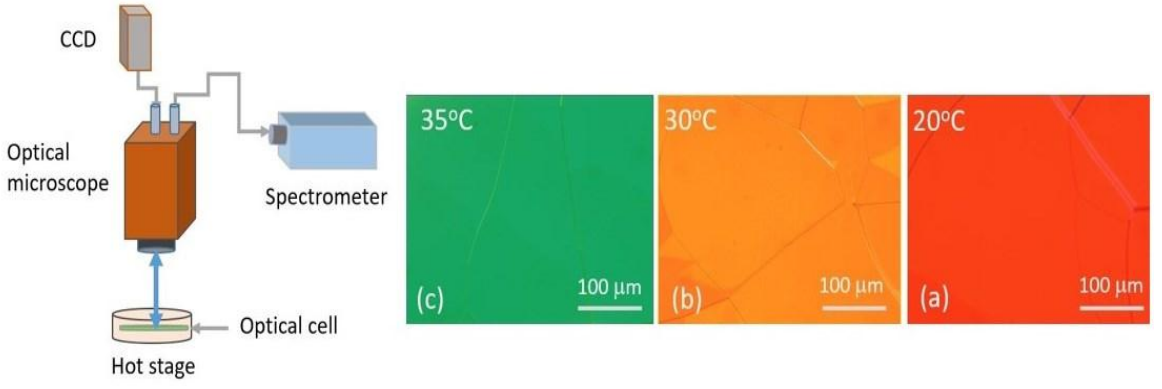

Fig. 3. The experimental setup and the microscope photos of the CLC mixture at different temperatures. As the temperature rises, the color of the CLC structure changes from red to greenish-blue

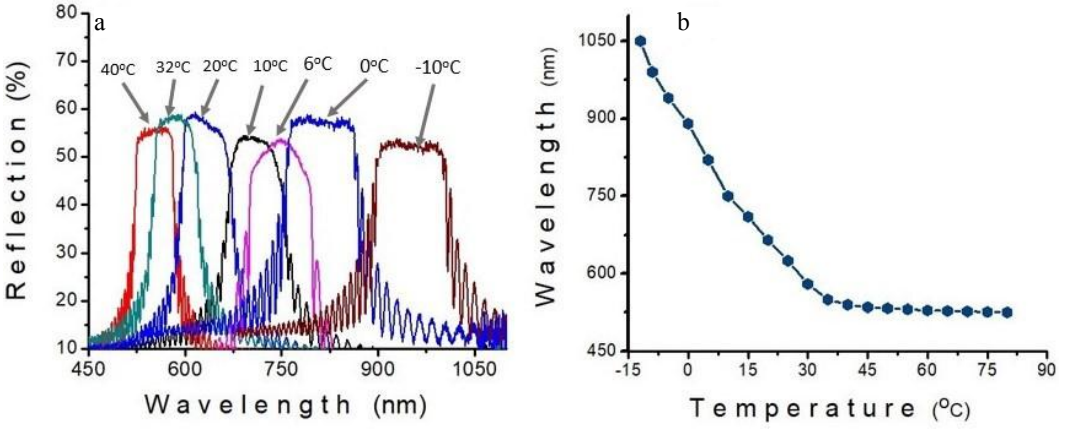

Fig. 4. Temperature-dependent tuning of the central wavelength of the SRBs recorded with a spectrometer (a), and the graphical presentation of this dependence (b)

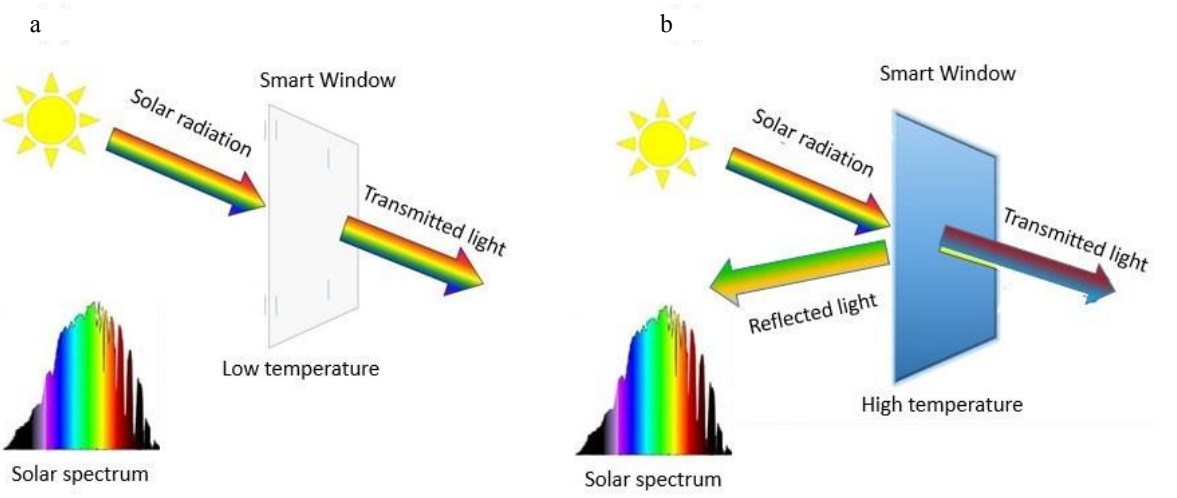

Fig. 5. The operation principle of the proposed CLCSW. The CLCSW is transparent at low temperatures, and solar radiation is transmitted in the building (a); one portion of the solar radiation is reflected from the CLCSW and the other one is transmitted through it at high temperatures (b)

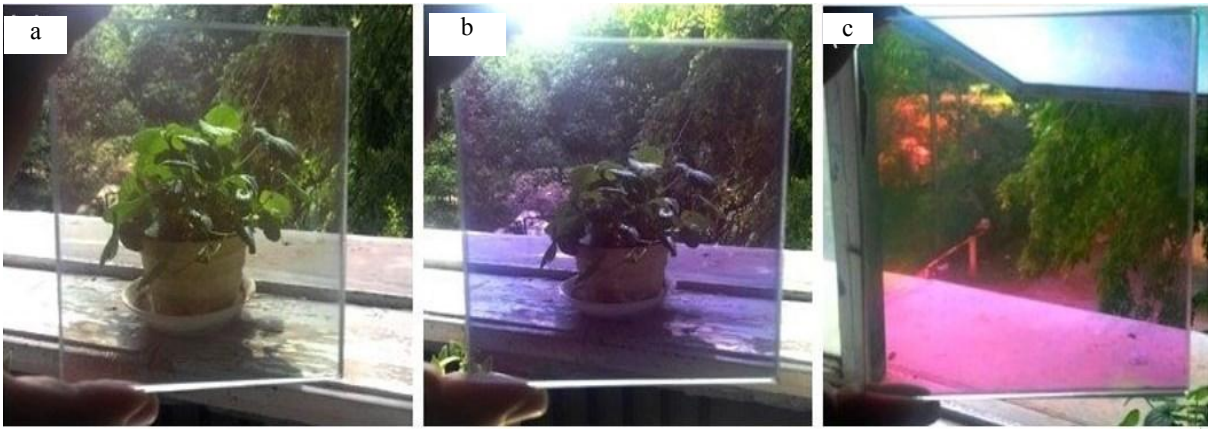

Fig. 6. Temperature-dependent color change of the CLCSW at variable ambient temperatures: (a) $t \leq 12$ °C, (b) $t = 20–25$ and (c) $t \geq 30–35$

We tested the thermo-optical properties of the CLCSW at variable ambient temperatures. At 12 ^{o}C, the CLCSW is transparent. At 20–25 ^{o}C, it becomes bluish-purple (reflects the red part of solar radiation), and at 30–35 ^{o}C and higher, it becomes reddish (reflects the yellow-green ranges of solar radiation, Fig. 6). It should be noted that the high and low temperatures indicated are relative, and can be adjusted on request, which is achieved by selecting the percentages of the CLC mixture components.

Fig. 7 shows the photo of the CLCSW reflecting the part of an outdoor scene (the University of Calabria, "UNICAL", Italy). The reflected images from the CLCSW are uniform and undistorted, indicating an even distribution of CLC structure over the entire area. The outdoor temperature is about 32 ^{o}C.

To estimate the effectiveness of the CLCSW it is necessary to measure the solar radiation intensity that the smart window blocks. For this purpose, we carried out experiments in which the CLCSW was oriented in such a way that the angle of incidence Q, between the solar radiation and the surface of the CLCSW, was 90 degrees. The light transmitted through the CLCSW was measured using a spectrometer and a solar power meter. Since the intensity of the ambient solar radiation varies by latitude and altitude, depending on seasons and time of day, and with cloud cover, the doses of solar radiation intensity were measured on an unclouded day in the summer months at solar noon, in Tbilisi (Georgia), with the coordinates: latitude – 41.7151° N, longitude – 44.8271° E. Fig. 8 shows the spectral distribution of solar radiation intensity. In particular, Fig. 8, *a* shows the solar spectrum transmitted inside the building without attenuation, and Fig. 8, *b* displays the attenuated solar spectrum intensity caused by the reflection from the CLCSW.

Fig. 7. CLCSW photos showing exterior views at an ambient temperature of 32 °C

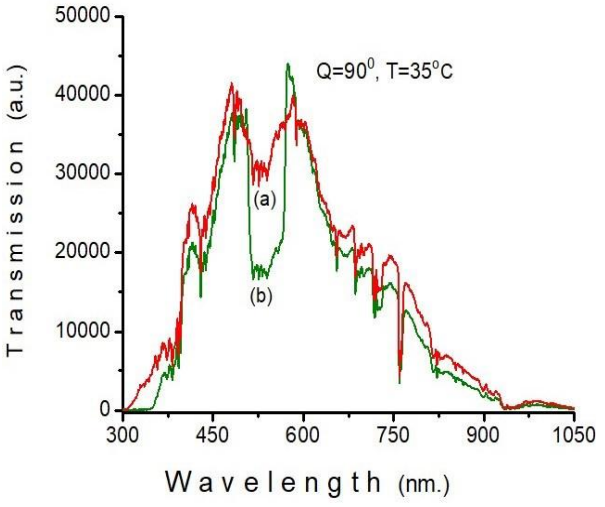

Fig. 8. The spectrum of solar radiation transmitted inside the building, (a) without attenuation, (b) reflected from the CLCSW

To calculate the solar radiation intensity reflected from the CLCSW, we use the method of integration of input data from the origin software, and to enhance the precision of the obtained results, we averaged the measurements based on day-to-day experiments, using Eq. (1):

$$I_0(\lambda,t)-I_1(\lambda,t)=t\int_{\lambda_i}^{\lambda_j} I_0(d\lambda)-t\int_{\lambda_i}^{\lambda_j} I_1(d\lambda)=$$

$$=35^oC[\int_{\lambda_{350nm}}^{\lambda_{1050nm}} I_0(d\lambda)-\int_{\lambda_{350nm}}^{\lambda_{1050nm}} I_1(d\lambda)]\ , \qquad (1)$$

where λ_i and λ_j are the starting and ending spectral points of the UV/VIS/NIR spectrum. Then we calculated the total intensity of solar radiation reflected from the CLCSW, which was equal to 23.5 %.

$$I_0(\lambda,t)-I_1(\lambda,t)/I_0(\lambda,t)\times 100=23.5\% \qquad (2)$$

Next, we measured the solar radiation transmitted through the CLCSW using a solar power meter. The intensity of the reflected solar radiation was quantitatively in good agreement with the results obtained by the spectral measurements. An important issue related to smart windows is their durability. The thermo-optical parameters of the CLCSW were tested for three years. For this purpose, the CLCSW was built into the frame and mounted on a stand. Monitoring of the thermo-optical behavior of the SRBs was carried out once a month. It was found that the temperature dependence of the SRB shift has undergone little change over the three years. In particular, at the given temperatures, there was an insignificant shifting of the SRBs toward the short-wave ranges of the optical spectrum (Fig. 9).

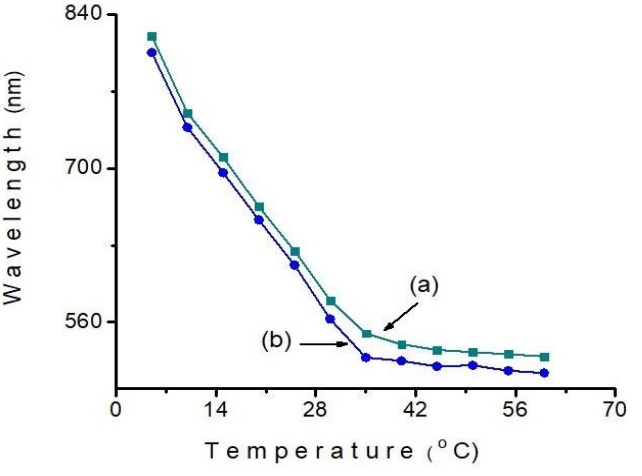

Fig. 9. Temperature-dependent shift of SRBs of CLC immediately after the assembly of CLCSW (a) and the temperature-dependent tuning of SRBs of CLCSW after the three years of operation (b)

It is worth noting that the proposed design of the CLCSW integrates the following advantages: (a) first and foremost, it reflects light, and the reflection is environmentally controllable, *i. e.*, the low-temperature window is transparent and reflects the different wavelengths of the solar spectrum following the ambient temperature variation; (b) intelligently controls the natural light; (c) CLCSW has high stability with UV-VIS-NIR light radiation and with temperature variation; (d) it provides a real-time response to a thermal stimulus; (e) the spectral location of the SRBs can be modified according to daytime, season, and geographic area; (f) CLCSW has simple fabrication technology and cost-effective exploitation behavior without using electricity and hard-wired control systems; (g) it has a broadband operating temperature interval of (–12 +80) ^{o}C; (h) it is safe, non-toxic, and humidity-resistant.

4. Conclusions

In summary, we developed a novel next-generation smart window prototype, the operation principle of which is based on such distinguishing properties of the CLCs as the temperature-controlled tuning of the SRBs. The concentration ratio of the CLC mixture compounds is chosen so that at low ambient temperatures the SRBs reflect the spectral part of solar radiation with low intensities, and at high ambient temperatures, they reflect solar spectral range with high intensities, enhancing the operational efficiency of the CLCSW. Moreover, we show that the proposed CLCSW reflects 23.5 % of total solar radiation intensity, which can significantly impact the interior temperature in living and working spaces and will help combat climate change. The easy-to-fabricate, polymerization-free technology of the CLCSW shows a real potential for the fabrication of smart windows, granted with such advanced behaviors as self-controlled real-time dynamicity upon the external thermal stimulus and operational longevity.

Acknowledgments

The financial support of the Shota Rustaveli National Scientific Foundation of Georgia (Project # FR-22-2543) is gratefully acknowledged.

References

[1] Santamouris, M.; Vasilakopoulou, K. Present and Future Energy Consumption of Buildings: Challenges and Opportunities towards Decarbonization. *e-Prime - Advances in Electrical Engineering, Electronics and Energy* **2021**, *1*, 100002. https://doi.org/10.1016/j.prime.2021.100002

[2] Niu, Y.; Zhou Y.; Du, D.; Ouyang, X.; Yang, Z.; Lan, W.; Fan, F.; Zhao, S.; Liu, Y.; Chen, S.; Li, J.; and Q. Xu. Energy Saving and Energy Generation Smart Window with Active Control and Antifreezing Functions. *Adv. Sci*. **2022**, *9*, 2105184. https://doi.org/10.1002/advs.202105184

[3] Ariosto, T.; Memari, A. M.; Solnosky, R. L. Development of Designer Aids for Energy Efficient Residential Window Retrofit Solutions. *Sustainable Energy Technol. Assess*. **2019**, *33*, 1–13. https://doi.org/10.1016/j.seta.2019.02.007

[4] Amirkhani, S.; Bahadori-Jahromi, A.; Mylona, A.; Godfrey, P.; Cook, D. Impact of Low-E Window Films on Energy Consumption and CO_2 Emissions of an Existing UK Hotel Building. *Sustainability* **2019**, *11*, 4265. https://doi.org/10.3390/su11164265

[5] Moghaddam, S.A.; Mattsson, M.; Ameen, A.; Akander, J.; Gameiro Da Silva, M.; Simões, N. Low-Emissivity Window Films as an Energy Retrofit Option for a Historical Stone Building in Cold Climate. *Energies* **2021**, *14*, 1–28. https://doi.10.3390/en14227584

[6] Lampert, C.M. Large-Area Smart Glass and Integrated Photovoltaics. *Sol. Energy Mater. Sol. Cells* **2003**, *76*, 489– 499. https://doi.org/10.1016/S0927-0248(02)00259-3

[7] Georg, A.; George, A.; Graf, W.; Wittwer, V. Switchable Windows with Tungsten Oxide. *Vacuum* **2008**, *82*, 730–735. https://doi.10.1016/j.vacuum.2007.10.020

[8] Badour, Y.; Jubera, V.; Andron, I.; Frayret, C.; Gaudon, M. Photochromism in Inorganic Crystallised Compounds. *Opt. Mater*. **2021**, *12*, 100110. https://doi.org/10.1016/j.omx.2021.100110

[9] Zhang, J.; Zou, Q.; and Tian, H. Photochromic Materials: More Than Meets the Eye. *Adv. Mater*. **2013**, *25*, 378–399. https://doi.org/10.1002/adma.201201521

[10] Zou, Y.; Yi, T.; Xiao, Sh.; Li, F.; Li, Ch.; Gao, X.; Wu, J.; Yu, M.; Huang, Ch. Amphiphilic Diarylethene as a Photoswitchable Probe for Imaging Living Cells. *J. Am. Chem. Soc*. **2008**, *130*, 15751–1575. https://doi.org/10.1021/ja8043163

[11] Jaik, Th. G.; Ciubini, B.; Frascella F.; and Jonas, U. Thermal Response and Thermochromism of Methyl Red-Based Copolymer Systems – Coupled Responsiveness in Critical Solution Behaviour and Optical Absorption Properties. *Polym. Chem*. **2022**, *13*, 1186–1214. https://doi.org/10.1039/D1PY01361K

[12] Somani, P. R.; Radhakrishnan, S. Electrochromic Materials and Devices: Present and Future. *Mater. Chem. Phys*. **2002**, *77*, 117–133. https://doi.org/10.1016/S0254-0584(01)00575-2

[13] Han, M.; Cho, Ch. H.; Jang, H.; Kim, E. Black-to-Transparent Electrochromic Capacitive Windows Based on Conjugated Polymers. *J. Mater. Chem. A* **2021**, *9*, 16016–16027. https://doi.org/10.1039/D1TA02996G

[14] Bouas-Laurent, H.; Durr, H. Organic Photochromism. *Pure Appl. Chem*. **2001**, *73*, 639–665. http://dx.doi.org/10.1351/pac200173040639

[15] Wiedemann, U.; Alt, W.; Meschede, D. Switching Photochromic Molecules Adsorbed on Optical Microfibers. *Opt. Express* **2012**, *20*, 12710–12720. https://doi.org/10.1364/OE.20.012710

[16] Mukbaniani, O.; Tatrishvili, T.; Pachulia, Z.; Londaridze, L.; Pirtskheliani, N. Quantum-Chemical Modeling of Hydrosilylation Reaction of Triethoxysilane to Divinylbenzene. *Chem. Chem. Technol.* **2022**, *16*, 499–506. https://doi.org/10.23939/chcht16.04.499

[17] Mukbaniani, O.; Brostow, W.; Aneli, J.; Londaridze, L.; Markarashvili, E.; Tatrishvili, T.; Gencel, O. Wood Sawdust Plus Silylated Styrene Composites with Low Water Absorption. *Chem. Chem. Technol.* **2022**, *16*, 377–386. https://doi.org/10.23939/chcht16.03.377

[18] Mukbaniani, O.; Aneli, J.; Tatrishvili, T.; Markarashvili, E.; Londaridze, L.; Kvinikadze, N.; Kakalashvili, L. Wood Polymer Composite Based on a Styrene and Triethoxy(Vinylphenethyl)silane. *Chem. Chem. Technol.* **2023**, *17*, 35–44. https://doi.org/10.23939/chcht17.01.035
[19] Mukbaniani, O.; Tatrishvili, T.; Kvinikadze, N.; Bukia, T.; Pachulia, Z.; Pirtskheliani, N.; Petriashvili; G. Friedel-Crafts Reaction of Vinyltrimethoxysilane with Styrene and Composite Materials on Their Base. *Chem. Chem. Technol.* **2023**, *17*, 325–338. https://doi.org/10.23939/chcht17.02.325
[20] Mukbaniani, O.; Tatrishvili, T.; Kvinikadze, N.; Bukia, T.; Pirtskheliani, N.; Makharadze, T.; Petriashvili; G. Bamboo-Containing Composites with Environmentally Friendly Binders. *Chem. Chem. Technol.* **2023**, *17*, 807–819. https://doi.org/10.23939/chcht17.04.807
[21] Huang, Y.; Zhou, Y.; Doyle, C.; Wu, Sh.-Ts. Tuning the Photonic Band Gap in Cholesteric Liquid Crystals by Temperature Dependent Dopant Solubility. *Opt. Express* **2006**, *14*, 1236–1242. https://doi.org/10.1364/OE.14.001236
[22] Ritacco, T.; Aceti, D. M.; Domenico, G. De.; Giocondo, M.; Mazzulla, A.; Cipparrone, G.; and Pagliusi, P. Tuning Cholesteric Selective Reflection In Situ Upon Two-Photon Polymerization Enables Structural Multicolor 4D Microfabrication. *Adv. Optical Mater*. **2022**, *10*, 1–9. https://doi.org/10.1002/adom.202101526
[23] Lu, H. B.; Xie, X. Y.; Xing, J.; Xu, C.; Wu, Z. Q.; Zhang, G. B.; Lv, G. Q.; Qiu, L. Z. Wavelength-Tuning and Band-Broadening of a Cholesteric Liquid Crystal Induced by a Cyclic Chiral Azobenzene Compound. *Opt. Mater. Express* **2016**, *6*, 3145–3158. https://doi.org/10.1364/OME.6.003145
[24] Xiang, J.; Li, Y.; Li, Q.; Paterson, D. A.; Storey, J. M. D.; Imrie, C. T.; Lavrentovich, O. D. Electrically Tunable Selective Reflection of Light from Ultraviolet to Visible and Infrared by Heliconical Cholesterics. *Adv. Mater*. **2015**, *27*, 3014–3018. https://doi.org/10.1002/adma.201500340
[25] Jing, T. Selective Reflection of Cholesteric Liquid Crystals. *Science Insights* **2022**, *40*, 515–517. https://doi.org/10.15354/si.22.re051
[26] Saadaoui, L.; Petriashvili, G.; De Santo, M. P.; Hamdi, R.; Othman, T.; Barberi, R. Electrically Controllable Multicolor Cholesteric Laser. *Opt. Express* **2015**, *23*, 22922–22927. https://doi.org/10.1364/OE.23.022922
[27] Chilaya, G.; Chanishvili, A.; Petriashvili, G.; Barberi, R.; Bartolino, R.; Cipparrone, G.; Mazzulla, A.; Shibaev, P. V. Reversible Tuning of Lasing in Cholesteric Liquid Crystals Controlled by Light-Emitting Diodes. *Adv. Mater*. **2007**, *19*, 565–568. https://doi.org/10.1002/adma.200600353
[28] Qu, R.; Li, G. Overview of Liquid Crystal Biosensors: From Basic Theory to Advanced Applications. *Biosensors* **2022**, *12*, 205. https://doi.org/10.3390/bios12040205
[29] Petriashvili, G.; Japaridze, K.; Devadze, L.; Zurabishvili, C.; Sepashvili, N.; Ponjavidze, N.; De Santo, M. P.; Matranga, M. A.; Hamdi, R.; Ciuchi, F.; *et al*. Paper Like Cholesteric Interferential Mirror. *Opt. Express* **2013**, *21*, 20821–20830. https://doi.org/10.1364/OE.21.020821
[30] Chen, Ch.-W.; Brigeman, A. N.; Ho, Ts.-J.; Khoo, I.C h. Normally Transparent Smart Window Based on Electrically Induced Instability in Dielectrically Negative Cholesteric Liquid Crystal. *Optical Material Express* **2018**, *8*, 691–697. https://doi.org/10.1364/OME.8.000691
[31] Tseng, H.-Yi.; Chang, Li-M.; Lin, K.-W.; Li, Ch.-Ch.; Lin, W.-H.; Wang, Ch.-T.; Lin, Ch.-W.; Liu Sh.-H.; Lin, Ts.-H. Smart Window with Active-Passive Hybrid Control. *Materials* **2020**, *13*, 4137. https://doi.org/10.3390/ma13184137
[32] Shen, W.; Li, G. Recent Progress in Liquid Crystal-Based Smart Windows: Materials, Structures, and Design. *Laser Photonics Rev*. **2023**, *17*, 2200207. https://doi.10.1002/lpor.202200207
[33] Zhang, R.; Zhang, Z.; Han, J.; Yang, L.; Li, J.; Song, Z.; Wang, T.; Zhu, J. Advanced Liquid Crystal-Based Switchable Optical Devices for Light Protection Applications: Principles and Strategies. *Light Sci Appl* **2023**, 12, 11. https://doi.org/10.1038/s41377-022-01032-y
[34] An, C-H.; Choi, T-H.; Oh, S-W. Energy-Efficient Liquid Crystal Smart Window with a Clear View. *Crystals* **2023**, *13*, 1464. https://doi.org/10.3390/cryst13101464

Received: February 03, 2024 / Revised: March 18, 2024 / Accepted: May 28, 2024

РОЗУМНЕ ВІКНО НА ОСНОВІ ХОЛЕСТЕРИЧНОГО РІДКОКРИСТАЛІЧНОГО ДЗЕРКАЛА, КЕРОВАНЕ ТЕМПЕРАТУРОЮ НАВКОЛИШНЬОГО СЕРЕДОВИЩА

Анотація. *У статті описано невеликий прототип розумного вікна на основі термооптичних властивостей холестеричних рідких кристалів. Завдяки безполімерній конструкції виготовлене розумне вікно є прозорим і може відбивати певні порції видимого або інфрачервоного світла, не потребуючи зовнішнього джерела живлення, а, отже, його простіше встановити й експлуатувати. Запропонована технологія розумного вікна на основі холестеричного рідкокристалічного дзеркала дасть змогу зменшити витрати на енергоспоживання завдяки відбиттю надлишкового сонячного світла та теплопередачі, підвищуючи комфорт для мешканців будівель і споруд.*

Ключові слова: *розумні вікна, холестеричні рідкі кристали, регулювання температурою, відбиття світла.*